Journal of Asian Earth Sciences 73 (2013) 121–127

Contents lists available at SciVerse ScienceDirect

Journal of Asian Earth Sciences

journal homepage: www.elsevier.com/locate/jseaes

Receiver function analysis of crustal structure beneath the eastern Tibetan plateau

Xiaoming Xu [a,*], Zhifeng Ding [a], Danian Shi [b], Xinfu Li [c]

[a] Institute of Geophysics, China Earthquake Administration, Beijing 100081, China
[b] Institute of Mineral Resources, Chinese Academy of Geological Sciences, Beijing 100037, China
[c] School of Geophysics and Information Technology, China University of Geosciences, Beijing 100083, China

ARTICLE INFO

Article history:
Received 24 September 2012
Received in revised form 30 March 2013
Accepted 14 April 2013
Available online 28 April 2013

Keywords:
Eastern Tibetan plateau
Receiver function
Crustal thickness
Poisson's ratio

ABSTRACT

We measure the crustal structure beneath the eastern Tibetan plateau by analyzing three-component teleseismic data recorded at 252 stations from January 1, 2008 to March 31, 2011. Lateral variations of the crustal thickness and Poisson's ratio are obtained by using receiver function method. The thinnest crust is ~27 km in the south Yangtze craton and the deepest Moho (~70 km) is estimated in the eastern margin of the Tibetan plateau. The distribution of Poisson's ratio shows the heterogeneity that high Poisson's ratios ($\upsilon > 0.27$) are found in the Chuandian plateau, intermediate values ($0.24 \leqslant \upsilon \leqslant 0.27$) exhibit in the Ordos block, the Qilian orogen, the Qinling–Dabie orogen, the Songpan-Ganzi terrane and the Sichuan basin, and low values ($\upsilon < 0.24$) appear in the Yangtze craton. The higher Poisson's ratios ($\upsilon > 0.30$) in the southeastern margin of the Tibetan plateau can be considered as the evidence of the dominantly mafic composition or locally partial melting in crust. Our observations of the crustal thickness and Poisson's ratio beneath the eastern Tibetan plateau not only reveal the lateral inhomogeneity of the crustal structure, but also provide some constraints on the mechanism of uplift and crustal thickening of the Tibetan plateau.

1. Introduction

As an archetypical continent–continent collision, the India-Asia collision began about 50 Ma ago, and has resulted in uplift of the Tibetan plateau and at least 1500 km of crustal shortening within continental lithosphere (Molnar and Tapponnier, 1975; England and Houseman, 1989; Rowley, 1996;). The resulting deformation is characterized by major thickening of the underlying crust, the formation of a series of Cenozoic strike-slip faults, and eastward escape of the Tibetan plateau's crustal materials (England and Houseman, 1989; Royden et al., 1997, 2008; Clark and Royden, 2000; Tapponnier et al., 2001; Wang et al., 2001). Besides the Indian plate in the south, the Tibetan plateau is bounded by several continental blocks, such as the Tarim basin to the northwest, the Qaidam basin to the north, the Ordos block to the northeast and the Yangtze craton to the east (Fig. 1). This study area includes the eastern margin of the Tibetan plateau, the Ordos block and the Yangtze craton. The eastern Tibetan plateau is a transitional zone between the Tibetan plateau and Yangtze craton, which is featured by a steep topographic gradient and the South-North Seismic Zone (SNSZ) of China indicating the strong crustal deformation and interaction between them. The SNSZ is associated with high seismicity and tectonic activities. There are 62 earthquakes with magnitude over Ms. 6.0 occurred in the SNSZ since 1970s, and particularly the giant Wenchuan Ms. 8.0 earthquake of 12 May 2008 caused more than 70,000 deaths and huge economic loss. What caused the complicated ground deformation and crustal thickening in this region? Dose the eastward movement of the Tibetan plateau induce the higher level of the seismicity in the SNSZ? The crustal structures are needed to understand these questions.

Teleseismic receiver function technique is one of the powerful tools for geophysicists to obtain the crustal structure beneath the seismic stations (e.g., Langston, 1979; Kosarev et al., 1999; Zhu and Kanamori, 2000; Kind et al., 2002). Recently, the crustal and upper mantle structures beneath the eastern Tibetan plateau have been investigated by many geophysicists. Zhang et al. (2009, 2010) observed the variation of the crust-mantle boundary and the lithosphere–asthenosphere boundary by using receiver function method, and concluded that the crustal thickness increases about 20 km from the Sichuan basin to the eastern Tibet. Pan and Niu (2011) measured the Moho depth and crustal *Vp*/*Vs* ratio beneath the Ordos block and adjacent areas, and they pointed out that the Moho depth appears to correlate with the surface topography and the Poisson's ratio shows significant lateral variations. The lateral heterogeneous structure of the eastern Tibetan plateau is also determined by different seismic tomographic method (e.g., Huang et al., 2002; Wang et al., 2003; Yao et al., 2008; Li et al., 2009,

* Corresponding author. Tel.: +86 10 62456685.
E-mail address: xiaomingxu912@163.com (X. Xu).

1367-9120/$ - see front matter © 2013 Elsevier Ltd. All rights reserved.
http://dx.doi.org/10.1016/j.jseaes.2013.04.018

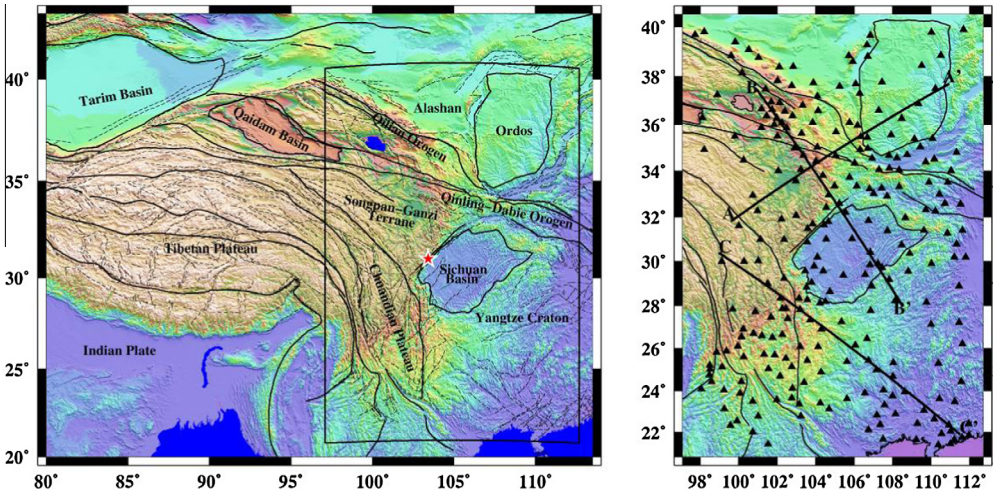

Fig. 1. Left: Map of the Tibetan plateau and the adjacent areas with the major tectonic features. The rectangular region shows the location of the study area. The red solid pentagram denotes the May 12, 2008 Wenchuan earthquake. Right: Topographic map showing the locations of seismic stations with the black triangles. The black thick lines are the profile lines of the CCP stacking shown in Fig. 5.

2012). In this paper, we use teleseismic P wave receiver function to estimate the crustal thickness and Poisson's radio in the study area. Then we will discuss the kinematics and dynamics of the interaction between the Tibetan plateau and its adjacent blocks based on the variation of crustal structure.

2. Data and method

With the rapid expansion of the broadband digital seismographs deployed by the China Earthquake Administration in recent years (Zheng et al., 2009), we assembled the three-component seismic waveforms recorded by 252 stations from 13 provincial network (Fig. 1) between January 1, 2008 and March 31, 2011. A total of 504 earthquakes with body wave magnitude greater than 5.5 and epicentral distance ranging from 30° to 90° were selected based on their signal to noise ratio (SNR). These earthquakes present reasonably good back azimuth coverage (Fig. 2) that could reduce influence from lateral crustal structural variations on our result analysis. The time-domain iterative deconvolution (Ligorria and Ammon, 1999) was used to compute radial receiver functions. Meanwhile, we took advantage of the Gaussian low-pass filter that the filter factor was set to 3.0 to suppress the noise in high frequency. We also removed the receiver functions that the fitting rate was less than 90% in the time-domain iteration. After visual examination, we obtained 22362 receiver functions with high SNR. There are about 88 receiver functions for each station in average.

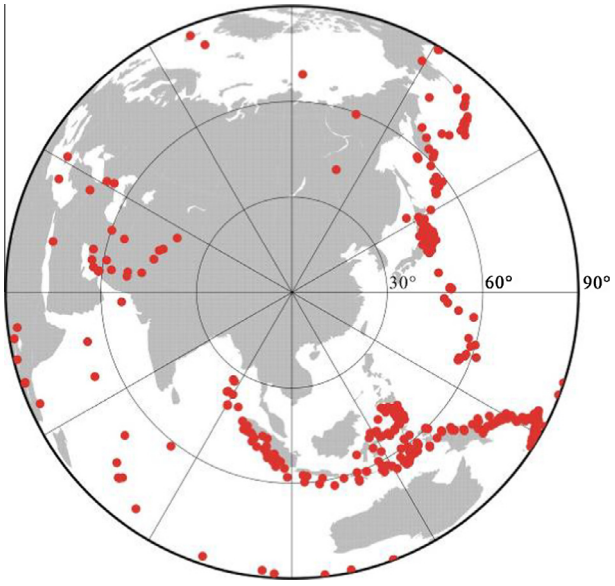

Fig. 2. Locations of earthquakes with epicentral distances of 30–90° used in this study.

The H-κ stacking method developed by Zhu and Kanamori (2000) was employed to determine the crustal thickness (H) and the ratio of P and S wave velocities (Vp/Vs ratio, or κ) under each seismic station. With a priori assumption on the average crustal P wave velocity (Vp), we can determine the crustal thickness and Vp/Vs ratio according to a grid search of the most energetic stack of the weighted receiver function amplitudes of the Moho converted Ps and reverberated PpPs and PpSs + PsPs phases. Thus, initial crustal averaged Vp is a key parameter in the H-κ stacking. Zhu and Kanamori (2000) showed that a 5% uncertainty in Vp produces the variation of H about 2 km and κ only varied by no more than 0.05 when the change of Vp is between 6.0 and 7.0 km/s. We therefore could see that H and, especially, κ are less sensitive to Vp. Comprehensively considering the previous wide-angle reflection results by Liu et al. (2006) and Wang et al. (2007), we adopted 6.3 km/s of Vp for deriving H and κ measurements in this study area. In H-κ stacking, the weighting factors for Ps, PpPs and PpSs + PsPs phases were assigned to 0.5, 0.3 and 0.2, respectively. Finally, we measured all the values of H and κ beneath each station, and the Poisson's radio (υ) was estimated from κ with empirical formula $\upsilon = 0.5 \times [1-1/(\kappa^2 - 1)]$. Fig. 3 shows the receiver functions and H-κ stacking results at three representative stations.

We also applied the approach of the common conversion point (CCP) migration with P wave receiver functions (Kind et al., 2002; Wittlinger et al., 2004; Shi et al., 2009) to image the crustal and upper mantle structure. We firstly migrated the receiver functions into spatial locations in a three-dimensional volume along ray paths calculated based on a layered velocity model (Vp = 6.3 km/s, and Vs = 3.6 km/s for the crust (Liu et al., 2006; Wang et al., 2007) and Vp = 8.1 km/s, and Vs = 4.47 km/s for the mantle below 65 km depth). Then all these receiver functions were normal projected and stacked to the vertical cross-section to produce a structural image. The amplitude of each pixel represented the impedance of the various interface such as the Moho discontinuity.